universe

IMPACT FACTOR 2.5

CITESCORE 4.3

Article

The Algorithm of the Two Neutron Monitors for the Analysis of the Rigidity Spectrum Variations of Galactic Cosmic Ray Intensity Flux in Solar Cycle 24

Krzysztof Iskra, Marek Siluszyk and Witold Wozniak

MDPI

https://doi.org/10.3390/universe10080311

universe

MDPI

Article

The Algorithm of the Two Neutron Monitors for the Analysis of the Rigidity Spectrum Variations of Galactic Cosmic Ray Intensity Flux in Solar Cycle 24

Krzysztof Iskra [1], Marek Siluszyk [1,2,*] and Witold Wozniak [3]

[1] Faculty of Aviation, Polish Air Force University, 08-521 Deblin, Poland; k.iskra@law.mil.pl
[2] Faculty of Sciences, Siedlce University, 08-110 Siedlce, Poland
[3] Polish Gas Company, 02-235 Warsaw, Poland; witold.wozniak@psgaz.pl
* Correspondence: m.siluszyk@law.mil.pl

Abstract: The method of the two neutron monitors was used to analyze the parameters of the rigidity spectrum variations (RSV) of galactic cosmic ray intensity (GCR) flux in solar cycle 24 based on the data from the global network of neutron monitors. This method is an alternative to the least squares method when there are few monitors working stably in a given period, and their use in the least squares method is impossible. Analyses of the changes in exponent γ in the RSV of GCR flux from 2009 to 2019 were studied. The soft RSV (γ = 1.2–1.3) of the GCR flux around the maximum epoch and the hard RSV (γ = 0.6–0.9) around the minimum epoch of solar activity (SA) is the general feature of GCR modulation in the GeV energy scale (5, 50), to which neutron monitors were found to correspond. Therefore, various values of the RSV γ in the considered period show that during the decrease and increase period of SA, the essential changes in the large-scale structure of the heliospheric magnetic field (HMF) fluctuations/turbulence take place. The exponent γ of the RSV of the GCR flux can be considered a significant parameter to investigate the long-period changes in the GCR flux.

Keywords: galactic cosmic ray (GCR) flux; algorithm of the two neutron monitors; rigidity spectrum variations (RSV); long-period variations in GCR

Citation: Iskra, K.; Siluszyk, M.; Wozniak, W. The Algorithm of the Two Neutron Monitors for the Analysis of the Rigidity Spectrum Variations of Galactic Cosmic Ray Intensity Flux in Solar Cycle 24. *Universe* **2024**, *10*, 311. https://doi.org/10.3390/universe10080311

Academic Editor: Peng-Fei Chen

Received: 11 June 2024
Revised: 27 July 2024
Accepted: 28 July 2024
Published: 30 July 2024

1. Introduction

GCR flux varies in different timescales. The experimental data of GCR show that the appearance of the peaks and plateaus observed in the long-term GCR variations in the heliosphere is not due to drifts of particles in it [1]. An interesting mechanism was proposed to explain the long-time variation. It was demonstrated that the exponent γ of the RSV $\delta D(R)/D(R)$, where ($\delta D(R)/D(R) \propto R^{-\gamma}$), is determined by the index α, ($\gamma \propto \alpha$). Because $\alpha = 2 - \nu$, we have ($\gamma \propto 2 - \nu$). Thus, the exponents γ and ν are closely related, and ν is the exponent of the Power Spectrum Density (PSD) of the HMF turbulence ($PSD \propto f^{-\nu}$) [2–8].

In subsequent work of this group, the universality of changes in the RSV of GCR flux in subsequent cycles of SA was confirmed, that is, that the RSV of GCR flux, i.e., at SA maxima, the spectrum is soft and at minima, it is hard. According to the close connection between the RSV of the GCR flux and the PSD of the HMF turbulence, through exponents of γ and ν, we argue that there is a radical rearrangement of the magnetic structures of the HMF turbulence in various regions of the heliosphere during the increases and decreases in the SA. Thus, at maxima of the SA, the efficient size of the HMF turbulence structure causing diffusion is smaller than the Larmor radius (LR) of the particle and the diffusion coefficient ($\chi_{II} \propto R^{\alpha}$) [4] and the corresponding mean free path of the particles strongly depend on the rigidity ($\chi_{II} \propto R^{1.2.3}$). Furthermore, in the minima of SA, the HMF turbulences structures change in such a way that their sizes are comparable to the LR of the GCR particles. During these periods, weak dependence of the diffusion coefficient on the rigidity ($\chi_{II} \propto R^{0.3-0.9}$) is observed, and particles with higher energies can be included in the modulation process [9].

In this work, for the first time, the method of two neutron monitors with different cut-off rigidities for determining the γ parameter was described in detail. Based on this parameter, variations' amplitudes of the GCR flux in the heliosphere in the 24th SA cycle were determined. In addition, the RSV of the GCR flux in the γ function at the maximum and minimum of SA are presented. The determined γ parameter can be implemented in the model of GCR particle transport in the heliosphere. The two-monitor method and the least squares method give similar results and confirm universal RSV changes in different periods of solar activity. The least squares method is presented in detail in Ref. [6].

2. Two-Station Method for Determining Rigidity Spectrum Exponent γ of the GCR Intensity Variation

The rigidity spectrum of long-term variations in the intensity of GCR is studied using a network of neutron monitors, which, to some extent, covers the entire surface of the Earth and registers particles in a wide range of energies. The accurate determination of the spectrum parameters encounters significant difficulties associated with instrumental effects, lack of continuity, and homogeneity in the data series, as well as significant errors in determining the spectrum during periods of minima of SA when the amplitude of variation is insignificant (Appendix A).

Variations in the intensity of cosmic rays can be classified based on the formula describing the intensity of cosmic rays recorded on Earth:

$$I_c^i(h_0). = \int_{R_c}^{\infty} D(R) m^i(R, h_0) dR, \quad (1)$$

where I is the intensity of the GCR component of type i at a point with cut-off rigidity R_c and pressure h_0; $m^i(R, h_0)$ is the integral generation factor, i.e., the number of registered particles of type i from one primary particle with rigidity R; $D(R)$ is the differential spectrum of primary cosmic rays as a function of rigidity. Varying (1) with respect to $m^i(R, h_0)$, R_c, and $D(R)$ we obtain

$$\delta I_c^i(h_0) = \int_{R_c}^{\infty} \delta D(R)\ m^i(R, h_0) dR + \int_{R_c}^{\infty} D(R)\ \delta m^i(R, h_0)\ dR + \int_{R_c}^{\infty} D(R)\ m^i(R, h_0)\ \delta dR, \quad (2)$$

The third term of Expression (2) is equal to

$$\int_{R_c}^{\infty} D(R)\ m^i(R, h_0)\ \delta dR = \delta \int_{R_c}^{\infty} D(R)\ m^i(R, h_0)\ dR = -D(R_c)\ m^i(R_c, h_0) \delta R_c.$$

To find the relative variations of GCR, we divide the left and right sides of Expression (2) by $I_c^i(h_0)$ [10,11] then, we obtain

$$\frac{\delta I_c^i(h_0)}{I_c^i(h_0)} = \frac{\int_{R_c}^{\infty} \delta D(R)\ m^i(R, h_0) dR}{I_c^i(h_0)} + \frac{\int_{R_c}^{\infty} D(R)\ \delta m^i(R, h_0)\ dR}{I_c^i(h_0)} - \frac{\delta dR_c\ D(R)\ m^i(R, h_0)}{I_c^i(h_0)}. \quad (3)$$

By introducing the so-called coupling coefficient between the primary cosmic ray component and the secondary component of type i,

$$W_c^i(R, h_0) = \frac{D(R)\ m^i(R, h_0)}{I_c^i(h_0)}$$

into Formula (3), we obtain

$$\frac{\delta I_c^i(h_0)}{I_c^i(h_0)} = \int_{R_c}^{\infty} \frac{\delta D(R)}{D(R)} W_c^i(R, h_0) dR + \int_{R_c}^{\infty} \frac{\delta m^i(R, h_0)}{m^i(R, h_0)}\ W_c^i(R, h_0) dR - \delta R_c W_c^i(R_c, h_0) \quad (4)$$

Formula (4) contains different variations of cosmic rays. And so, the first term means extraterrestrial variations, primarily associated with the activity of the Sun. The second and third terms of this formula mean terrestrial variations associated with meteorological

effects and the Earth's magnetic field. These are the most important variations with which you can study electromagnetic conditions in interplanetary space. To determine RSV, we take only the first term of the Formula (4). The second and third terms of Formula (4) can be neglected because we use experimental data corrected on meteorological effects, and for high-energy particles, the geomagnetic effects are very small. Based on the above assumptions, Equation (4) is simplified into (5).

$$\frac{\delta I_c^i(h_0)}{I_c^i(h_0)} = \int_{R_c}^{\infty} \frac{\delta D(R)}{D(R)} W_c^i(R, h_0) dR. \quad (5)$$

The RSV ($\frac{\delta D(R)}{D(R)}$) of the 11-year period of the GCR flux has a power law form and can be represented as follows [10]

$$\frac{\delta D(R)}{D(R)} = \begin{cases} AR^{-\gamma}, R \leq R_{max} \\ 0, \quad R > R_{max} \end{cases}, \quad (6)$$

where R is the rigidity of the particles; R_{max} is the upper rigidity limit of modulation; γ and A are the exponent and power of the RSV of GCR flux, respectively.

This work is a continuation of research on the RSV of the GCR flux conducted for over 40 years for the last 5 cycles of SA.

In previous papers [6,9] temporal changes in the power law RSV of the long-term variations in the GCR in various periods of SA from 1965 (start of 20th cycle) to 2009 (start of 24th cycle), was shown.

The hard RSV of the GCR flux for the minimum period and a soft RSV, based on the NMs data (1965–2012), are connected with the different relationships to the diffusion coefficient in rigidity function for various epochs of SA. This dependence is weaker in the minimum period of SA than in the maximum period of SA. It is related to a radical rearrangement of the magnetic structures of the HMF turbulence from the minima to the maxima epoch of SA.

In the variation in the flux of GCR of the i-th secondary component of GCR at the observation point with the geomagnetic cut-off rigidity Rc, in addition to isotropic variations, there is also a contribution from the 1st and 2nd harmonics of the GCR anisotropy. However, statistically, the changes in GCR anisotropy are insignificant compared to the changes in the isotropic intensity, and, therefore, the variations in the intensity of the neutron monitor can be represented as follows [12,13].

Substituting Expression (6) into (5) we obtain

$$\frac{\delta I_c^i(h_0)}{I_c^i(h_0)} = \int_{R_c}^{\infty} AR^{-\gamma} W_c^i(R, h_0) dR, \quad (7)$$

where $W_c^i(R, h_0)$ is the coupling function depending on the height h_0 and R—the rigidity of the primary GCR particles at the observation point.

In this work, to determine the exponent γ of the RSV of the GCR flux and its changes in the 24th cycle of SA (2009–2019), the two-station method was used (the year 2009 was accepted as the reference point, which corresponds to the maximum of GCR intensity).

The algorithm of the two-station method consists of calculating the ratios of the amplitudes according to the data of two stations with different geomagnetic thresholds, R_{1c} and R_{2c}, of the primary GCR particles [14]. The amplitudes of variations in the secondary component of GCR corrected for meteorological effects are expressed as follows:

$$\left(\frac{\delta I}{I}\right)_1 = \int_{R_{1c}}^{R_{max}} AR^{-\gamma} W_1(R, h_1) dR, \quad (8)$$

$$\left(\frac{\delta I}{I}\right)_2 = \int_{R_{2c}}^{R_{max}} AR^{-\gamma} W_2(R, h_2) dR. \quad (9)$$

$A_1 = \left(\frac{\delta I}{I}\right)_1$ and $A_2 = \left(\frac{\delta I}{I}\right)_2$ are the amplitudes of GCR variations at different observation stations; $W_1(R, h_1)$ and $W_2(R, h_2)$ are the corresponding coupling coefficients between the primary and secondary components of GCR. By inserting the introduced notation, we have

$$\mathrm{A}_1 = A\int_{R_{1c}}^{R_{max}} R^{-\gamma} W_1(R, h_1) dR, \tag{10}$$

$$\mathrm{A}_2 = A\int_{R_{2c}}^{R_{max}} R^{-\gamma} W_2(R, h_2) dR. \tag{11}$$

From Expressions (10) and (11), we can obtain variation amplitude in the interplanetary space.

$$A = \frac{\mathrm{A}_1}{\int_{R_{1c}}^{R_{max}} R^{-\gamma} W_1(R, h_1) dR} \tag{12}$$

$$A = \frac{\mathrm{A}_2}{\int_{R_{1c}}^{R_{max}} R^{-\gamma} W_2(R, h_2) dR}. \tag{13}$$

From Expressions (12) and (13), we conclude that the amplitude of variation in interplanetary space should be the same for monitors with different cut-off rigidities in terms of the correctness of calculations. If we divide Expressions (10) and (11), we obtain

$$\frac{A_1}{A_2} = \frac{\int_{R_{1c}}^{R_{max}} R^{-\gamma} W_1(R, h_1) dR}{\int_{R_{2c}}^{R_{max}} R^{-\gamma} W_2(R, h_2) dR}. \tag{14}$$

Let us introduce the following notation:

$$K_1 = \int_{R_{1c}}^{R_{max}} R^{-\gamma} W_1(R, h_1) dR, \;\; K_2 = \int_{R_{1c}}^{R_{max}} R^{-\gamma} W_2(R, h_2) dR. \tag{15}$$

These so-called integral coupling coefficients are taken from [14].

Substituting (15) into (14), we see that the ratio of the amplitudes of the two stations is equal to the ratio of the corresponding integral coupling coefficients:

$$\frac{A_1}{A_2} = \frac{K_1}{K_2}. \tag{16}$$

3. Experimental Results and Discussion

Two pairs of neutron monitors, Oulu–Potchefstroom (O-P) and Apatity–Mexico (A-M), were used to calculate the RSV exponent γ of the GCR flux with the two-station method.

Let us introduce the notations A_O, A_p, A_A, A_M; K_o, K_p, K_A, K_M as the amplitudes of variations and integral coupling coefficients from neutron monitors Oulu, Potchefstoom, Apatity, and Mexico, respectively.

The changes in the GCR flux variation for pairs Oulu–Potchefstroom and Apatity–Mexico neutron monitor data on the Earth's surface are presented in Figure 1a,b. Figure 1a,b shows a difference between the GCR flux registered on the Earth by two pairs of NMs with various cut-off rigidities.

Based on Equation (16) for the appropriate pairs of amplitudes (A_O, A_p, A_A, A_M) of the flux variation for neutron monitors and their corresponding integral coupling coefficients, we can write

$$\frac{A_P}{A_O} = \frac{K_P}{K_O}, \;\; \frac{A_M}{A_A} = \frac{K_M}{K_A}. \tag{17}$$

In Table 1, we present the ratios of the amplitudes A_O, A_p, A_A, A_M of variations for two pairs of monitors for the 24th solar cycle (2009–2019).

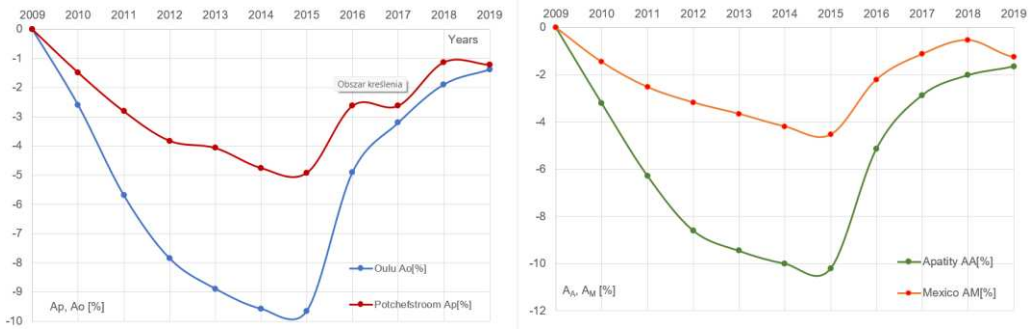

(**a**) (**b**)

Figure 1. (**a**,**b**) The changes in the GCR flux variation for NMs (**a**) Oulu–Potchefstroom data, and the same changes for (**b**) Apatity–Mexico at Earth for the period of 2009–2019 (the year 2009 was accepted as the reference point).

Table 1. The amplitudes A_O, A_p, A_A, A_M and ratios of the amplitudes $\frac{A_P}{A_O}$, $\frac{A_M}{A_A}$ for two pairs of monitors for 24th solar cycle (2009–2019).

Year	A_P	A_O	A_P/A_O	A_M	A_A	A_M/A_A
2009	0	0	---	0	0	---
2010	-1.48 ± 0.50	-2.59 ± 0.11	0.57 ± 0.12	-1.46 ± 0.08	-3.20 ± 0.06	0.45 ± 0.10
2011	-2.81 ± 0.20	-5.69 ± 0.03	0.49 ± 0.07	-2.52 ± 0.04	-6.28 ± 0.02	0.40 ± 0.07
2012	-3.82 ± 0.10	-7.85 ± 0.01	0.49 ± 0.05	-3.17 ± 0.02	-8.59 ± 0.01	0.37 ± 0.05
2013	-4.07 ± 0.09	-8.89 ± 0.01	0.46 ± 0.04	-3.65 ± 0.02	-9.45 ± 0.01	0.39 ± 0.04
2014	-4.75 ± 0.08	-9.58 ± 0.01	0.50 ± 0.04	-4.19 ± 0.01	-9.99 ± 0.01	0.42 ± 0.04
2015	-4.92 ± 0.06	-9.65 ± 0.01	0.51 ± 0.04	-4.53 ± 0.01	-10.2 ± 0.01	0.44 ± 0.03
2016	-2.62 ± 0.18	-4.89 ± 0.03	0.54 ± 0.06	-2.20 ± 0.03	-5.14 ± 0.02	0.43 ± 0.05
2017	-2.62 ± 0.26	-3.20 ± 0.06	0.82 ± 0.07	-1.12 ± 0.14	-2.86 ± 0.06	0.39 ± 0.10
2018	-1.13 ± 0.62	-1.89 ± 0.12	0.60 ± 0.07	-0.53 ± 0.36	-2.02 ± 0.11	0.26 ± 0.06
2019	-1.22 ± 2.17	-1.38 ± 0.22	0.89 ± 0.49	-1.24 ± 0.07	-1.64 ± 0.16	0.76 ± 0.15

From Table 1, we see that the errors of the amplitudes of GCR intensity variation and their respective ratios are large in the SA minima, and for the NM in Potchefstroom, the error value exceeds the value of the amplitude in 2019. This is due to the data instability and missing data during certain months.

Table 2 presents the coupling coefficients and the corresponding γ parameter for four monitors at maximum, minimum, and average solar activity for maximum modulation rigidity 200 GV.

Table 2. Coupling coefficients K_P, K_O, K_M, K_A for 4 values of gamma exponent (0.0; 0.5; 1.0; 1.5) and for R_{max} 200 GV, where min—minimum, av—average, and max—maximum determine periods of the SA [14].

R = 200 GV	K_P			K_O			K_M			K_A		
γ	min	av	max	min	av	max	min	av	max	min	av	max
0.0	0.8748	0.8555	0.8362	0.8803	0.8534	0.8264	0.8686	0.8556	0.8426	0.8803	0.8534	0.8264
0.5	0.6148	0.5932	0.5716	0.8063	0.7455	0.6846	0.5452	0.5328	0.5203	0.8063	0.7455	0.6846
1.0	0.4905	0.4688	0.4471	0.9395	0.8237	0.7078	0.3820	0.3712	0.3603	0.9395	0.8237	0.7078
1.5	0.4258	0.4043	0.3828	1.3303	1.1008	0.8713	0.2889	0.2796	0.2702	1.3303	1.1008	0.8713

Based on the results from Table 2, we determine the dependence of the coupling coefficients on the γ parameter by means of approximation with a polynomial of the second degree at the maximum, minimum, and average of the SA. The relationships are shown in Figure 2a–d.

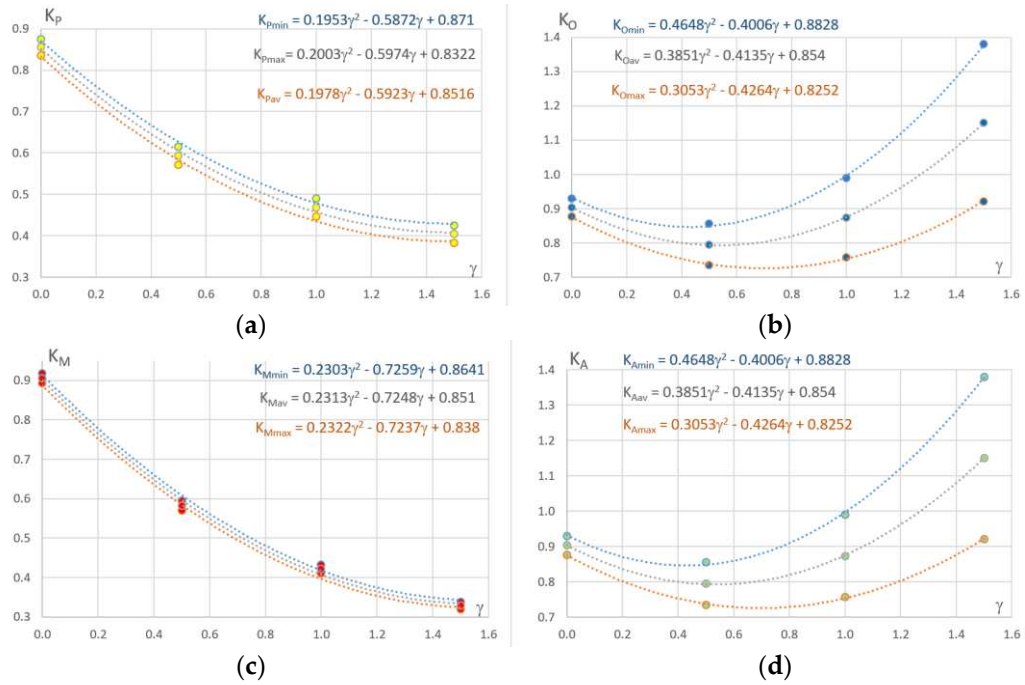

Figure 2. (**a**–**d**) Coupling coefficients (**a**) K_P, (**b**) K_O, (**c**) K_M, and (**d**) K_A in the γ function at minimum average and maximum SA.

Based on the results from Table 3, we determine the dependence of the ratios of the coupling coefficients of the respective pairs of monitors and their average values on the γ parameter by means of approximation with linear functions at the maximum, minimum, and average of the SA and the inverse dependence (see Figures 3a,b and 4a,b).

Table 3. Presents the ratios of the coupling coefficients $\frac{K_P}{K_O}$ and $\frac{K_M}{K_A}$ for 4 values of γ parameters (0.0; 0.5; 1.0; 1.5) and for R_{max} = 200 GV, where min—minimum, av—average, max—maximum determine periods of the SA [14].

R_{max} = 200 GV	**K_P/K_O**			**K_M/K_A**		
γ	**min**	**av**	**max**	**min**	**av**	**max**
0.0	0.994	1.003	1.012	0.987	1.003	1.020
0.5	0.762	0.796	0.835	0.676	0.718	0.760
1.0	0.522	0.569	0.632	0.407	0.458	0.509
1.5	0.320	0.367	0.439	0.217	0.264	0.310

To determine the γ parameter from 2009–2019, we put in dependencies γ as a function of the ratios of the coupling coefficients, the magnitudes of ratios of the amplitudes of the respective pairs of monitors, and their average values using Equation (17). In turn, Table 4 RSV exponent γ of the GCR flux in 2009–2019 and corresponding coupling coefficients for four monitors determined from the equations in Figure 2a–d, respectively.

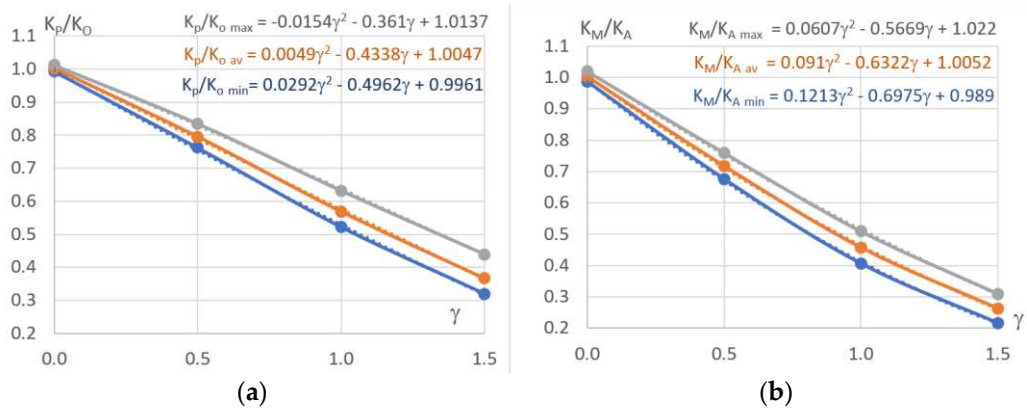

(**a**) (**b**)

Figure 3. (**a**,**b**) The ratios of the coupling coefficients of the respective pairs of monitors and their average values on the γ parameter: (**a**) K_P/K_O; (**b**) K_M/K_A.

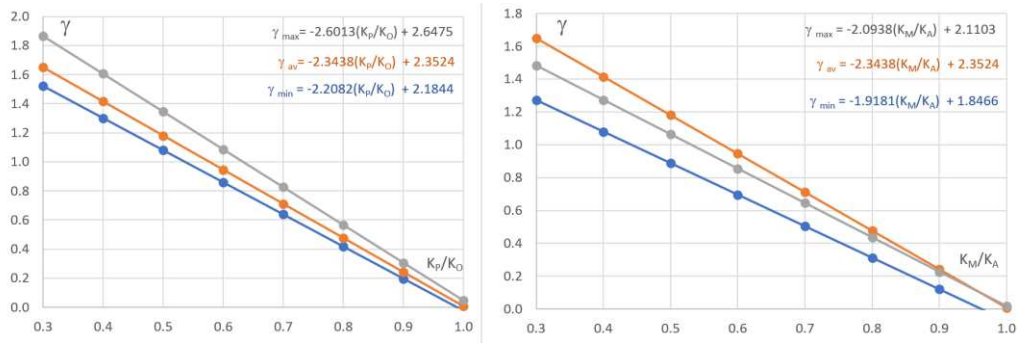

(**a**) (**b**)

Figure 4. (**a**,**b**) The exponent γ as a function of the ratios of the coupling coefficients of the respective pairs of monitors and their average values: (**a**) γ(K_P/K_O); (**b**) γ (K_M/K_A).

Table 4. Rigidity spectrum variations exponent γ of the GCR flux and the corresponding coupling coefficients for Apatity (K_A), Oulu (K_O), Potchefstroom (K_P), Mexico (K_M) in the years 2009–2019 determined from the equations in Figure 2a–d, respectively.

YEAR	γ(P-O)	γ(M-A)	K_O	K_P	K_A	K_M
2010	0.91 ± 0.26	0.92 ± 0.20	0.90	0.50	0.91	0.39
2011	1.09 ± 0.16	1.04 ± 0.14	1.00	0.46	0.97	0.36
2012	1.12 ± 0.12	1.21 ± 0.09	1.02	0.44	0.92	0.31
2013	1.27 ± 0.11	1.29 ± 0.08	0.78	0.40	0.78	0.29
2014	1.36 ± 0.11	1.21 ± 0.08	0.81	0.39	0.76	0.30
2015	1.32 ± 0.11	1.15 ± 0.07	0.80	0.39	0.74	0.31
2016	1.26 ± 0.14	1.07 ± 0.11	0.94	0.42	0.85	0.34
2017	1.15 ± 0.16	1.06 ± 0.19	1.03	0.45	0.98	0.35
2018	0.99 ± 0.16	0.71 ± 0.12	0.94	0.48	0.83	0.47
2019	0.94 ± 1.09	0.34 ± 0.28	0.92	0.49	0.80	0.65

Figure 5 presents changes in the RSV exponent γ of GCR flux in 2009–2019 (cycle 24 of SA) determined from the equations in Figure 4a,b, respectively.

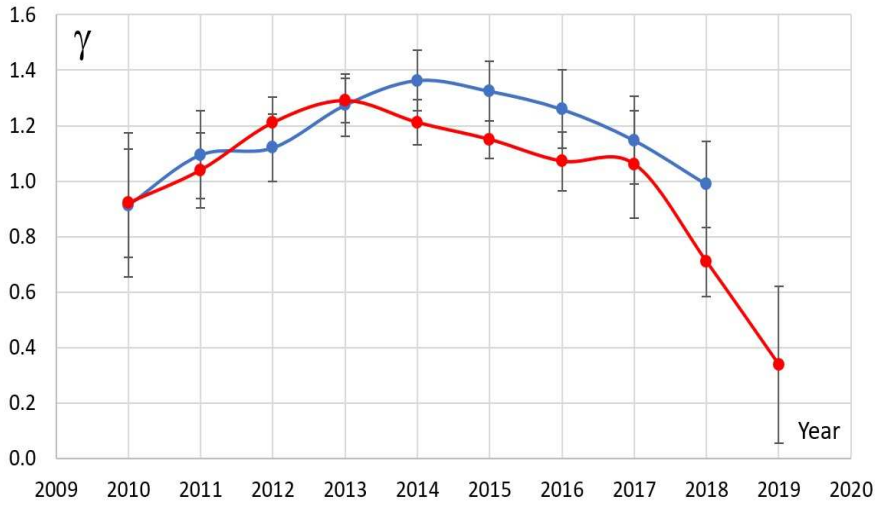

Figure 5. The temporal changes in the RSV exponent γ of GCR flux [where $\gamma(K_P/K_O)$—blue curve; $\gamma(K_M/K_A)$—red curve] for the period 2009–2019 (2009 accepted as a reference point) [6].

Based on the results from Table 4, we determine amplitudes of the variations in the GCR flux for four monitors in the heliosphere at 1 AU, at the ecliptic plane outside of Earth's magnetosphere after the corrections according to Formulas (12) and (13) and shown in Figure 6.

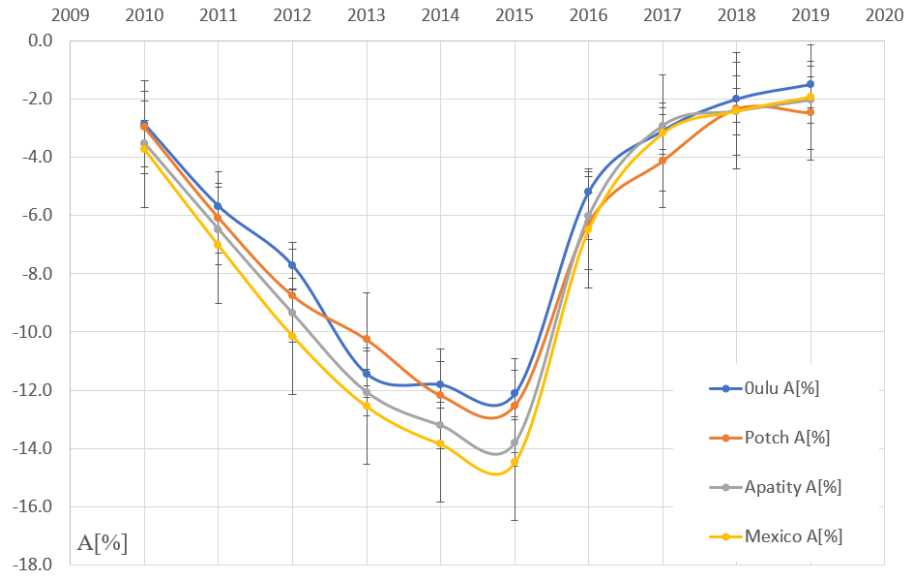

Figure 6. Changes in GCR flux variations in Oulu and Potchefstroom and Apatity and Mexico NMs data after recalculation to the heliosphere for the period 2009–2019 (2009 accepted as a reference point) [6].

Figure 6 shows no difference between Oulu and Potchefstroom and Apatity and Mexico NMs data in terms of correctness of calculations.

According to the power law character with the exponent γ of the RSV (the exponent γ in the minimum is smaller than in the maximum of SA), the variation in the GCR flux descends more slowly in the minimum than in the maximum of SA.

This means that particles with higher energy are included in the modulation process because of the changes in the structure of the HMF turbulences.

4. Conclusions

(i) Based on the method of two stations for two pair monitors (Oulu–Potchefstroom and Mexico–Apatity), the changes in the RSV exponent γ of the GCR flux in the 24th cycle of solar activity were obtained. In solar activity minima and around the minima, the γ exponent varies in a range γ = 0.6–0.9, while in the SA maxima and in the vicinity, the gamma exponent changes in the range γ = 1.2–1.3;

(ii) The RSV of GCR isotropic flux is soft in the SA maxima and in the vicinity of the SA, while in the SA minima and in the vicinity of the SA, it is hard in the considered period from 2009 to 2019. Thus, the universality of the temporal changes in the RSV of GCR isotropic flux for all 11 cycles of SA from 1965 to 2019 has been confirmed;

(iii) The results obtained indicate the change in the character of the diffusion of GCR during the decreasing and increasing epochs of SA caused by the changes in the structure of HMF turbulences. In the period of increasing SA, the RSV of the GCR flux quickly becomes soft (i.e., the exponent γ quickly reaches its maximum value: γ = 1.3, while in the period of decreasing SA, the rigidity spectrum gradually becomes hard (i.e., the γ gradually changes from 1.29 to 0.64);

(iv) The structural changes in HMF turbulence play a decisive role in the formation of long-term GCR variations in the heliosphere;

(v) The presented two-monitor method is an alternative to the least squares method when there are only a few monitors working stably in a given period. Because of the lack of data, we cannot use the least squares method;

(vi) The two-monitor method and the least squares method give similar results and confirm universal RSV changes in different periods of solar activity.

Author Contributions: K.I. and M.S. and W.W. worked on this paper. K.I. conceptualization, performing basic calculations, discussing the analysis of the obtained results. K.I. and M.S. methodology, conceived of the presented idea and wrote the main manuscript text, writing—original draft preparation, M.S. made part of numerical calculations, participation in the analysis and discussion and interpretation of the obtained results, prepared all figures, visualization; W.W. preparation of input data, verified the analytical methods, formal analysis, Authors discussed the results and contributed to the final manuscript. All authors have read and agreed to the published version of the manuscript.

Funding: This research received no external funding. The Polish Air Force Academy in Dublin will be the founder.

Data Availability Statement: Data is contained within the article. The original contributions presented in the study are included in the article, further inquiries can be directed to the corresponding author.

Conflicts of Interest: The authors declare no conflict of interest.

Appendix A. Calculation of Exponent γ by the Least Squares Method

We use neutron monitors experimental data to calculate temporal changes in the rigidity R spectrum exponent γ ($\frac{\delta D(R)}{D(R)} = AR^{-\gamma}$) of the 11-year variations in the GCR intensity in considered periods.

The rigidity R spectrum exponent γ of the 11-year variations in the GCR intensity was calculated using the thoroughly selected monthly average data of neutron monitors in periods, including four ascending and four descending phases of solar activity in the A > 0 and the A < 0 epochs. A criterion for the data selection was a continuous function of neutron monitors with different cut-off rigidities throughout the analyzed period. The magnitudes $J_i{}^k$ of the monthly average variations in the GCR intensity for 'i' neutron monitor were calculated as $J_i{}^k = \frac{N_k - N_0}{N_0}$; N_k is the running monthly average count rate (k = 1, 2, 3, ..., months), and N_0 is the monthly average count rate for the year of the maximum intensity (in the minimum epoch of solar activity); the count rate of the maximum intensity is accepted as the 100% level. The magnitudes J_i^k of the monthly average variations

of the GCR intensity measured by 'i' neutron monitor with the geomagnetic cut-off rigidity R_i and the average atmospheric depth h_i are defined as

$$J_i^k = \int_{R_i}^{R_{max}} \left(\frac{\delta D(R)}{D(R)} \right)_k W_i(R, h_i) dR, \quad \text{(A1)}$$

where $(\delta D(R)/D(R))_k$ is the rigidity spectrum of the GCR intensity variations for the k month; $W_i(R, h_i)$ is the coupling coefficient for the neutron component of GCR, and R_{max} is the upper limiting rigidity beyond which the magnitude of the GCR intensity variation vanished. For the power law rigidity spectrum $(\delta D(R)/D(R))_k = AR^{-\gamma_k}$, one can rewrite Equation (A1) as follows:

$$J_i^k = A_i^k \int_{R_i}^{R_{max}} R^{-\gamma_k} W_i(R, h_i)\ dR. \quad \text{(A2)}$$

where J_i^k is the observed magnitude at given month k, and A_i^k is the magnitude of the GCR intensity variations recalculated to the heliosphere (free space). From Equation (A2) we have

$$A_i^k = J_i{}^k / \int_{R_i}^{R_{max}} R^{-\gamma_k} W_i(R, h_i)\ dR. \quad \text{(A3)}$$

The values of the A_i^k should be the same (in the scope of the accuracy of the calculations) for any 'i' neutron monitor if the pairs of the parameters γ_k and Rmax are properly determined. A similarity of the values of the A_i^k for various neutron monitors is an essential argument to affirm that the data of the particular neutron monitor and the method of the calculations of γ_k are reliable.

To find the temporal changes in the rigidity spectrum exponent γ_k (k = 1, 2, 3, …, months), a minimization of the expression $\phi = \sum_i^n \Big(A_i^k - A^k)^2$ (where $A^k = \frac{1}{n}\sum_i^n A_i^k$ and n is the number of neutron monitors) has been provided. The values of the expression $\int_{R_i}^{R_{max}} R^{-\gamma_k} W_i(R, h_i)\ dR$ for the magnitudes of R_{max} (from 30 GV up to 200 GV with the step of 10 GV) and γ (from 0 to 2 with the step of 0.05) were found based on the method presented in this paper. The upper limiting rigidity R_{max}, beyond which the magnitude of the GCR intensity variation vanishes, equals 200 GV. This assumption is reasonable for the 11-year variation in the GCR intensity. Minimization of the expression ϕ for the smoothed monthly means (with the interval of 13 months) of the magnitudes of the 11-year variation in the GCR intensity has been provided with respect γ_k, for a given number of neutron monitors.

References

1. Stozhkov, Y.; Makhmutov, V.; Svirzhevsky, N. About Cosmic Ray Modulation in the Heliosphere. *Universe* **2022**, *8*, 558. [CrossRef]
2. Alania, M.V.; Modzelewska, R.; Wawrzynczak, A. Peculiarities of cosmic ray modulation in the solar minimum 23/24. *J. Geophys. Res. Space Phys.* **2014**, *119*, 4164. [CrossRef]
3. Bieber, J.W.; Matthaeus, W.H.; Smith, C.W.; Wanner, W.; Kallenrode, M.-B.; Wibberenz, G. Proton and electron mean free paths: The Palmer consensus revisited. *Astrophys. J.* **1994**, *420*, 294. [CrossRef]
4. Jokipii, J.R. Propagation of cosmic rays in the solar wind. *Rev. Geophys. Space Phys.* **1971**, *9*, 27–87. [CrossRef]
5. Melnikov, Y.P. General correlation scales of random component of IMF. *Geomagn. Aeoronomia* **2005**, *45*, 445.
6. Siluszyk, M.; Iskra, K.; Alania, M.V.; Miernicki, S. Interplanetary magnetic field turbulence and rigidity spectrum of the galactic cosmic rays intensity variation (1968–2012). *J. Geophys. Res.* **2018**, *123*, 30–38. [CrossRef]
7. Siluszyk, M.; Iskra, K. Modeling the Time Delay Problem of Galactic Cosmic Ray Flux in Solar Cycles 21 and 23. *Sol. Phys.* **2020**, *295*, 68. [CrossRef]
8. Toptygin, I.N. *Cosmic Rays in Interplanetary Magnetic Fields*; Dordrecht, D. Reidel Publishing Co.: Dordrecht, The Netherlands, 1985. Available online: https://link.springer.com/book/10.1007/978-94-009-5257-7 (accessed on 1 May 2024).
9. Alania, M.V.; Iskra, K. Features of the Solar Wind Large-Scale Structure in the Different Periods of Solar Activity Based on the Variations of Cosmic Rays. *Adv. Space Res.* **1995**, *16*, 241. [CrossRef]
10. Dorman, L.I. Cosmic ray variations, Moscow: State Publishing House for Technical and Theoretical Literature. *J. Phys. Soc. Jpn.* **1957**, *13*, 8. [CrossRef]
11. Dorman, L.I. *Cosmic Rays Variations and Space Explorations*; North-Holland: Amsterdam, The Netherlands, 1974.

12. Dorman, L.I. *Variations of Galactic Cosmic Rays*; Izdatel'stvo Moskovskogo Universiteta: Moscow, Russia, 1975; p. 214. Available online: https://ui.adsabs.harvard.edu/abs/1975MIzMU.....D/abstract (accessed on 1 May 2024). (In Russian)
13. Dorman, L.I. Cosmic ray long-term variation: Even-odd cycle effect, role of drifts, and the onset of cycle 23. *Adv. Space Res.* **2001**, *27*, 601–606. [CrossRef]
14. Yasue, S.; Mori, S.; Sakakibara, S.; Nagashima, K. *Coupling Coefficients of Cosmic Ray Daily Variations for Neutron Monitor Stations*; Report of Cosmic-Ray Research Laboratory: Nagoya, Japan, 1982.